

Investigation of a Circulation Controlled Cylinder Using an Adaptive Wall Wind Tunnel

Fabrizio A. Dionisio* and Alan Nurick[†]
University of the Witwatersrand, Johannesburg 2050, South Africa

An experimental investigation was carried out to characterize the two-dimensional performance of a circulation controlled (CC) cylinder with two slots and a removable flap. The tests were performed in an adaptive wall wind tunnel to minimize wall interference. The effects of slot pressure, slot width, freestream velocity, and a flap on the lift and drag coefficients were determined. It is shown that the lift and drag acting on the cylinder may be defined in terms of three flow phenomena, i.e., distortion of the flow by the geometry of the cylinder, momentum of the CC air, and the combined action of the circulation generated by the CC air and freestream velocity.

Nomenclature

C_D	=	$D/(0.5\rho U^2 D_c W)$, drag coefficient
C_L	=	$L/(0.5\rho U^2 D_c W)$, lift coefficient
C_P	=	$P/(\rho U^2)$, pressure coefficient
C_μ	=	$(\rho V^2 t)/(0.5\rho U^2 D_c)$, slot momentum coefficient
D	=	drag
D_c	=	cylinder outer diameter
F	=	force
L	=	lift
P	=	pressure in tail boom
t	=	total width of slots
U	=	freestream velocity
W	=	span of cylinder
V_j	=	jet velocity
Γ	=	circulation
ρ	=	air density

Subscripts

calc	=	calculated values
i	=	L for lift or D for drag
meas	=	measured data

Introduction

THE attachment of a jet to an adjacent convex surface was first described by Young¹ in 1800. The phenomenon was rediscovered by Coanda in about 1910 and has since been referred to as the “Coanda effect.” Attempts have been made to utilize the increased lift coefficients, which can be developed by circulation controlled (CC) aerofoils on both fixed- and rotary-wing aircraft. For fixed-wing aircraft Attinello² demonstrated that the Coanda effect applies to both high- and low-speed flows. A supersonic jet will adhere to a deflected wing flap, referred to as a “blown flap.” The blown flap has been implemented on aircraft including the British Aircraft Corporation’s TSR.2 (Ref. 3). CC tests were carried out on a scaled model of the wing of the Gruman A6-A (Ref. 4). CC has been applied to the lifting rotor of the Kaman CC helicopter⁵ and the stopped rotor of the U.S. Navy/DARPA X-Wing (Ref. 6). The use of CC on the tail boom of a helicopter, in conjunction with the downwash from the main rotor to develop an antitorque component, was proposed by Velazquez in 1971 (Ref. 7) and im-

plemented on the MD520N,⁸ MD Explorer,⁹ and Ka-26 (Ref. 10) helicopters.

Wind-tunnel tests were carried out on a number of CC elliptical^{11–15} and circular^{16–21} aerofoils with constant CC flows. The effects of pulsing the CC air were investigated experimentally.²² The performance of hovering rotors with CC cylindrical blades have been investigated on a test rig,^{23,24} as has CC helicopter tail booms in the wake of a hovering rotor.^{25–27}

The objective of this work was to identify flow mechanisms inherent in CC flowfields associated with circular cylinders located in the wakes of hovering rotors. Typically, total slot pressures of less than 7000 Pa are used in helicopter tail booms.^{25,28}

Lockwood¹⁷ measured the lift and drag characteristics of circular cylinders with a diameter of 150 mm, slot widths of 0.152 mm, and various slot combinations. The slot momentum coefficients ranged from 0 to 6 and freestream Reynolds numbers to 4.15×10^5 . Compressed air at high pressure was used for the CC air resulting in sonic air velocities from the slots. The lift and drag coefficients were related to C_μ for the configurations tested. No attempt was made to correlate the data using a more general term than C_μ .

Dunham¹⁸ carried out wind-tunnel tests to investigate the lift and drag of CC models with one and two slots. The models spanned the width of the wind tunnel. Corrections were made for wake blockage. The lift and drag coefficients were correlated using C_μ as Spence²⁹ showed it could be used to correlate blown flap data at different slot widths. It was concluded that this assumption is incorrect for circulation controlled cylinders (CCC). Also, drag data were difficult to correlate, which was attributed to the transitional Reynolds-number range of the tests. Tests were subsequently carried out on a helicopter CC rotor with cylindrical blades.²³

Logan²⁵ performed experiments on a CCC helicopter tail boom mounted under the main rotor of an OH-6A helicopter. The diameter of the tail boom varied linearly from 460 to 380 mm and had a single slot. Jet velocities varied from 36 to 68 m/s and slot widths from 4.3 to 19 mm. Velocity ratios V_j/U varied from 2.5 to 10 and C_μ from 0.2 to 1.2. The angular location of the slot was varied to optimize the tail boom torque, which was correlated with the velocity ratio and C_μ . Van Horn²⁶ showed that for CCC helicopter tail booms a second slot is required to keep the flow attached to the tail boom.

Berndt²⁰ measured the lift and drag acting on a CCC in an adaptive wall wind tunnel. The cylinder had four adjustable slots that spanned the cylinder. Tests were carried out with various slot combinations. Data were correlated against C_μ only.

Nurick and Groesbeek²⁷ noted from results obtained on a CCC tailboom located in the wake of a hovering rotor that the torque developed by a CCC could be related to three flow phenomena resulting in a more general description of the lift.

Experimental investigations of the boundary-layer flow on a CC body and the potential flow outside the boundary layer were made.

Received 6 April 1995; revision received 5 October 2000; accepted for publication 5 October 2000. Copyright © 2001 by the American Institute of Aeronautics and Astronautics, Inc. All rights reserved.

*Graduate Student, School of Mechanical Engineering, Branch of Aeronautical Engineering.

[†]Graduate Advisor, School of Mechanical Engineering, Branch of Aeronautical Engineering.

Wilson and Goldstein¹⁹ measured the effects of surface curvature on a two-dimensional wall jet, showing that the structure of a curved wall jet is not self preserving, the rate of decay of the maximum velocity being greater than that of a plane jet. Novak and Cornelius¹⁵ measured the velocity field of a CC aerofoil using a laser Doppler velocimeter and pressures on the Coanda surface. It was shown that while the flowfield is similar to other wall bounded jet flows the external freestream plays an important role in the overall mixing and structure of the wall flow. Shakouchi²¹ showed that for a jet to remain attached to a cylindrical surface the exit angle of the jet to the surface of the cylinder should be less than 25 deg.

In analytical investigations of circulation controlled flows,^{27,30-40} modeling of combined Coanda and external flows requires the use of two parameter turbulent shear-stress descriptions.^{27,40}

The lift developed by a CCC has in the past been related to the slot momentum coefficient C_μ only. This coefficient gives the ratio of the momentum of the air exiting from all of the slots of a cylinder to the dynamic head of the freestream and describes only one of the flow phenomena of a CCC.

An experimental program was initiated to characterize the macroscale performance of CC flows on a cylinder with particular reference to the flow phenomena identified by Nurick and Groesbeek.²⁷

Analytical Background

Any predictive capability for the performance of the CCC must describe flow effects including the following:

1) Distortion of the freestream is caused by nonsymmetrical disturbances on the cylinder such as the slots and flaps, as shown in Fig. 1, which run the full width of the airfoil. They result in circulation about the cylinder, and a lift component in addition to drag contribution.

2) Thrust is caused by momentum of the air flowing through the slots. This air will remain attached to the external surface of the cylinder as a result of the Coanda effect if the inclination of the nozzles to the external surface is less than 25 deg (Ref. 21). The direction of this thrust is a function of the exit angle and the manner in which it interacts with the external flow.

3) Combined effects of CC air and freestream velocity are the last flow effects. When both external and CC flows are present one can expect that lift and drag components arising from flow distortion and momentum of the CC air exist. These forces could be modified by their interaction. Also, the combined flows could result in additional lift and drag as a result of the interaction of the resulting circulation and the freestream velocity.

Lift and Drag Caused by Freestream Velocity Only

Air flowing over a cylinder will induce a drag force on the cylinder in the direction of the freestream. The coefficient of drag of a smooth cylinder with no circulation is a function of the Reynolds number⁴¹ only and has not been investigated in detail. The flap fixed to a cylinder, as shown in Fig. 1, which is normal to the flow, should result in a sharp point separation with the drag being a weak function of the Reynolds number.

Both the drag and lift acting on a cylinder may be expected to be a function of the freestream velocity, cylinder diameter, air density, air viscosity, and span. A dimensional analysis including these parameters gives

$$F_{li} = K_{li} \rho U^2 D_c W (\rho U D_c / \mu)^{a_i} (W/D_c)^{b_i} \quad (1)$$

where K_{li} would be a function of the geometrical features of the cylinder such as the widths and number of slots and flaps.

A regression analysis of the data showed that the lift is independent of the Reynolds Number; thus, $a_i = 0$. For long cylinders, or two-dimensional tests, the lift per unit span will be independent of the span of the cylinder; thus, $b_i = 0$. Thus

$$L_1 = K_{1L} \rho U^2 D_c W \quad (2)$$

and the drag is given by

$$D_1 = K_{1D} \rho U^2 D_c W \quad (3)$$

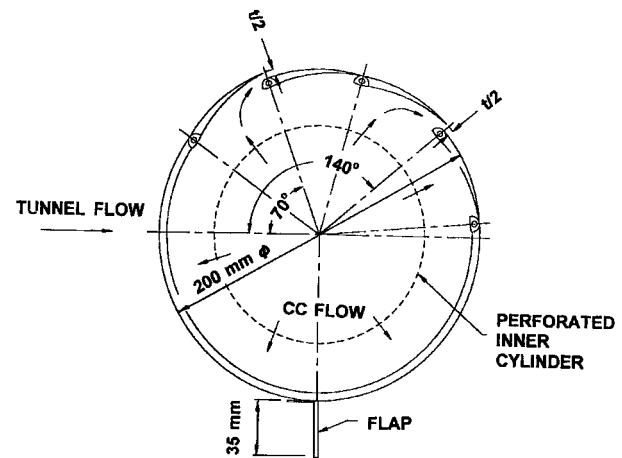


Fig. 1 Cylinder cross section.

Lift and Drag Caused by CC Air Only

The lift and drag in the absence of an external flow will be related to the momentum of the air and the angular point at which it leaves the cylinder. The axial velocity of the air in the cylinder is small compared to its exit velocity, and the flow through the slots is constant along its length. The force can be related to the pressure of the air in the tail boom, the total slot thickness, the cylinder diameter and span, the air density, and viscosity. Dimensional analysis gives the force acting on the cylinder as

$$F_{2i} = K_{2i} P D_c W (P \rho D_c^2 / \mu^2)^{c_i} (t/D_c)^{d_i} \quad (4)$$

where K_{2i} , c_i , and d_i are constants for a particular geometry.

The term $(P \rho D_c^2 / \mu^2)$ is a Reynolds number squared. Correlation of the data showed that the force acting on a cylinder is proportional to the boom pressure P and the slot total thickness t only; thus, $c_i = 0$, and the lift and drag forces caused only by momentum effects can be written respectively:

$$L_2 = K_{2L} P W t \quad (5)$$

and

$$D_2 = K_{2D} P W t \quad (6)$$

where the constants K_{2i} can be measured for each particular case.

Lift and Drag Caused by Freestream Velocity and Circulation Control Air

If the lift and drag attributable to the combined effects of freestream and CC air are functions of the freestream velocity, cylinder diameter, cylinder pressure, slot thickness, air density, and air viscosity, then it can be shown that

$$F_{3i} = K_{3i} \rho U^2 D_c W (\rho U D_c / \mu)^{e_i} (P / \rho U^2)^{f_i} (t/D)^{g_i} \quad (7)$$

A regression analysis of the data showed that F is independent of the Reynolds number, and because L and D are independent of the slot thickness then $e_i = g_i = 0$.

A value for f_i can be obtained by considering the lift given by

$$L_3 = \rho U \Gamma W \quad (8)$$

The circulation Γ is a function of the jet velocity, the geometry of the external velocity field, and the circumference of the cylinder. Thus, for a given flow geometry

$$\Gamma \propto V_j D_c \propto [2(P/\rho)]^{1/2} D_c \quad (9)$$

Substitution of Eq. (9) into Eq. (8) gives

$$L_3 \propto \rho U [2(P/\rho)]^{\frac{1}{2}} D_c W = \rho U^2 [2(P/\rho U^2)]^{\frac{1}{2}} D_c W \quad (10)$$

Comparison of Eqs. (7) and (10) indicates that $f_i = \frac{1}{2}$. Thus, Eqs. (7) can be written as

$$L_3 = K_{3L} \rho U^2 (P/\rho U^2)^{\frac{1}{2}} D_c W \quad (11)$$

and

$$D_3 = K_{3D} \rho U^2 (P/\rho U^2)^{\frac{1}{2}} D_c W \quad (12)$$

$$C_L/2 = K_{1L} + K_{2L} (P/\rho U^2) (t/D_c) + K_{3L} (P/\rho U^2)^{\frac{1}{2}} \quad (13)$$

Total Lift and Drag

When both the freestream and CC flow are present, the three flow phenomena will be present, but possibly modified by their interactions, altering the values of K_{1i} , K_{2i} , and K_{3i} . The coefficient of lift can then be written as

$$C_L/2 = K_{1L} + K_{2L} C_P (t/D_c) + K_{3L} C_P^{\frac{1}{2}} \quad (14)$$

The term $2K_{1L}$ is the lift coefficient attributed to flow distortion as a result of geometrical disturbances on the cylinder surface and could be defined in terms of a circulation about the cylinder and the uniform flowfield. Similarly, as just noted the third term can be defined in terms of the combined effects of a circulation about the cylinder and the uniform flowfield. The second term is related to the momentum of the CC air and consequent induced momentum changes of the freestream.

Similarly, the drag coefficient is given by

$$C_D/2 = K_{1D} + K_{2D} C_P (t/D_c) + K_{3D} C_P^{\frac{1}{2}} \quad (15)$$

for the case where the drag is not a function of the Reynolds number.

Because the slot momentum coefficient is given by

$$C_\mu = \frac{\rho V_j^2 t}{0.5 \rho U^2 D_c} = 4 \left(\frac{P}{\rho U^2} \right) \left(\frac{t}{D_c} \right) \quad (16)$$

it appears, by comparing Eqs. (13) and (16) that it is only the second term in Eq. (13) that is related to the slot momentum coefficient. Thus the forces acting on a CCC cylinder cannot be adequately described using only the slot momentum coefficient.

Experimental Equipment

Circulation Controlled Cylinder

The CCC is fitted with four individually adjustable slots that run across the span of the cylinder. The CCC spanned the width of the tunnel between the two fixed walls. CC air entered the cylinder through a duct on the floor of the tunnel. Circular perforated discs are located inside the cylinder to eliminate axial velocity components to ensure that the air emerges from the slots in a direction normal to the span. The outer diameter of the cylinder is 0.2 m. The flap was used in some of the tests.

A cross section of the CCC is presented in Fig. 1.

Adaptive Wall Wind Tunnel

The adaptive wall wind tunnel²⁰ is of the open type; a general arrangement is given in Fig. 2.

Each flexible wall is comprised of a 0.8-mm-thick galvanized sheet moved by 26 slides spaced at 100 mm. The walls are held against the slides by means of a pressure drop across the walls with the pressure on the external surface of the walls being reduced by a vacuum pump. The walls are positioned iteratively for each test using potential methods²⁰ to model the flow in terms of the measured lift and drag. The wall positions are assumed to have converged when the measured lift is equal to that predicted using potential flow methods.

Table 1 Range and standard deviations of transducers

Parameter	Range	Standard deviation
Cylinder lift, N	1500	1.96
Cylinder drag, N	750	1.42
Cylinder pressure, Pa	7500	9.0
Freestream velocity, m/s	55	0.5
Tunnel static pressure, Pa	2000	1.0

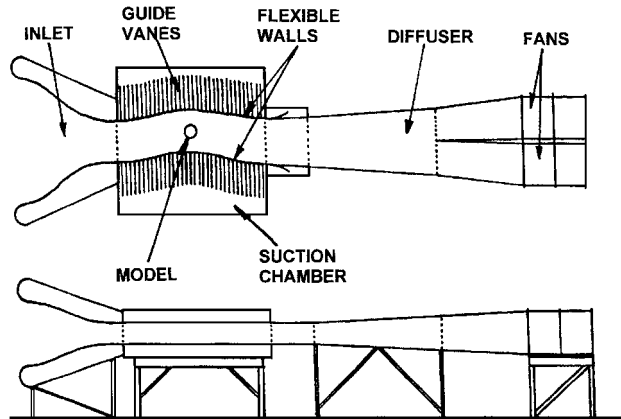


Fig. 2 General arrangement of adaptive wall wind tunnel.

The tunnel is fitted with a two-component balance to measure the lift and drag forces.

Experimental data were recorded using a computer. Each data point was averaged from 1000 readings.

Deviations from a two-dimensional flow around the cylinder were investigated by measuring the velocity downstream of the cylinder at a distance of $2.2D_c$, on a zero streamline, using a pitot tube. For this test the mean air velocity upstream of the cylinder was 25 m/s, $C_L = 2.4$, $C_D = 0.6$, and $C_\mu = 0.415$. The mean velocity of the air along the measurement line was 17.44 m/s, with a standard deviation of 0.24 m/s, to the edge of the boundary layer, which was approximately 10 mm thick.

Details of the range and accuracies of relevant transducers are presented in Table 1.

Experimental Procedure and Results

The experiments were designed such that the constants K_{ji} ($j = 1, 2, 3; i = L, D$) could be determined individually and also in combination using multiple linear regression for cylinders with and without a flap.

Lift and Drag Caused by Freestream Velocity Only

The ranges of the parameters over which the tests were carried out are given in Table 2. Tests were carried out with and without the flap fitted. The results are presented in Figs. 3 and 4. The results of the linear regression are presented in Table 3. As may be seen from the data in Table 3, Eqs. (2) and (3) can be used to describe the lift and drag acting on the cylinder in the absence of circulation control air.

The distortion of the flow will depend on all irregularities on the surface of the cylinder such as the flap and slot widths. As can be seen in Fig. 3, the flap has a marked effect on the lift and surface roughness represented by the slots. The slots, which are on the opposite side of the cylinder to that on which the flap is located, reduce the lift with the reduction being related to the thickness of the slots.

In Fig. 4 it can be seen that the slots alone will induce a negative lift with the decrease in lift again being related to the thickness of the slots. For the case of no flap, it would be expected that the lift would be zero at $t = 0$ and will decrease as t increases.

The variation of K_{1L} with the total slot width of both slots for the cylinder, with and without a flap, is shown in Fig. 5, and the values of the gradients are given in Table 4. As can be seen in

Table 2 Test ranges to obtain constants K_{1i}

Parameter	Range
U , m/s	10 to 40
P , Pa	0
t , mm	2 to 10

Table 5 Test ranges to obtain constants K_{2i}

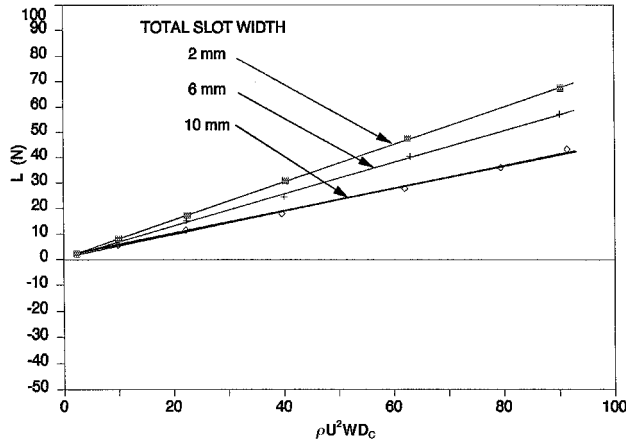
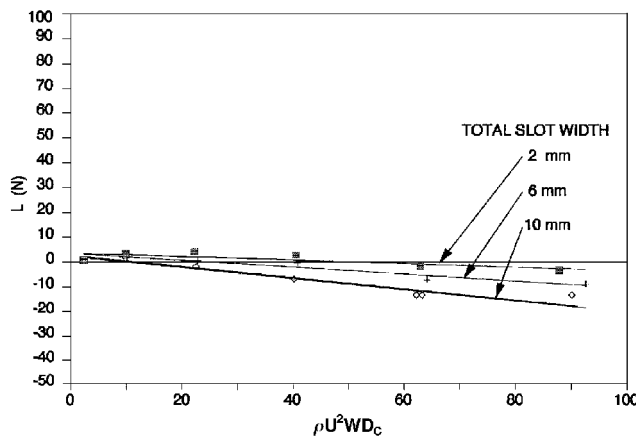
Parameter	Range
U , m/s	0
P , Pa	0 to 6000
t , mm	2 to 8

Table 3 Measured values of K_{1L} with and without a flap

Test condition, mm	K_{1L}	Correlation coefficient	Standard deviation, N
<i>Cylinder with flap</i>			
$t = 2$	0.734	0.9999	0.306
$t = 6$	0.618	0.9995	0.555
$t = 10$	0.446	0.998	0.813
<i>Cylinder with no flap</i>			
$t = 2$	-0.0711	0.7834	1.694
$t = 6$	-0.139	0.9596	1.198
$t = 10$	-0.222	0.9315	2.004

Table 4 Values of dK_{1L}/dt

Test condition	dK_{1L}/dt , m^{-1}	Correlation coefficient
With flap	-36.4	0.9938
No flap	-23.1	0.9694

Fig. 3 Variation of L with $\rho U^2 WD_c$ (cylinder with flap).Fig. 4 Variation of L with $\rho U^2 WD_c$ (cylinder with no flap).**Table 6** Measured values of K_{2L} with and without a flap

Test condition, mm	K_{2L}	Correlation coefficient	Standard deviation, N
<i>Cylinder with flap</i>			
$t = 2$	1.205	0.9847	0.324
$t = 6$	1.139	0.9986	0.287
$t = 10$	1.030	0.9978	0.309
$t = 2, 6$, and 10	1.016	0.9770	1.286
<i>Cylinder with no flap</i>			
$t = 2$	0.977	0.849	0.493
$t = 6$	0.993	0.9984	0.263
$t = 10$	1.041	0.999	0.312
$t = 2, 6$ and 10	0.967	0.9926	0.982
<i>Cylinders with and without a flap</i>			
$t = 2, 6$ and 10	0.988	0.9660	1.149 (all tests)

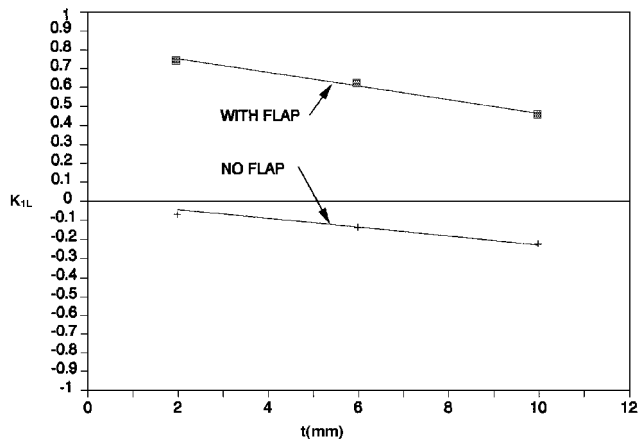
Fig. 5 Variation of K_{1L} with t for a cylinder with and without a flap.

Fig. 5, K_{1L} does vary with geometrical factors such as t , as would be expected. The gradients dK_{1L}/dt depend on whether a flap is fitted or not, indicating that the effects of the slot width on the generation of circulation cannot simply be added by assuming that flow superposition applies.

Lift and Drag Caused by Circulation Control Air Only

To determine the values of K_{2i} , the cylinder was rotated to a position where the air leaving the cylinder blew down the center of the tunnel, ensuring that no interference was caused by the air striking the walls. The forces were resolved to give the lift and drag forces acting on the cylinder with respect to the tunnel axes, had it been correctly orientated.

The ranges of the parameters over which the tests were carried out are given in Table 5. Each range of tests was carried out with and without the flap fitted. The results are presented in Fig. 6. Because the flap, in the absence of an external flow, was found to have no effect on the value of K_{2L} , all of the data is plotted on a single graph.

The data is presented in Table 6. Approximately 800 tests were run to obtain K_{2L} . For all of the results presented in Table 6, K_{2L} has a value of approximately unity. A value of unity for K_{1L} can be obtained from a momentum balance applied to a control volume, which includes the slot and in which it is assumed that the flow

Table 7 Test ranges to obtain constants K_{1L} , K_{2L} , K_{3L} , K_{1D} , K_{2D} , K_{3D}

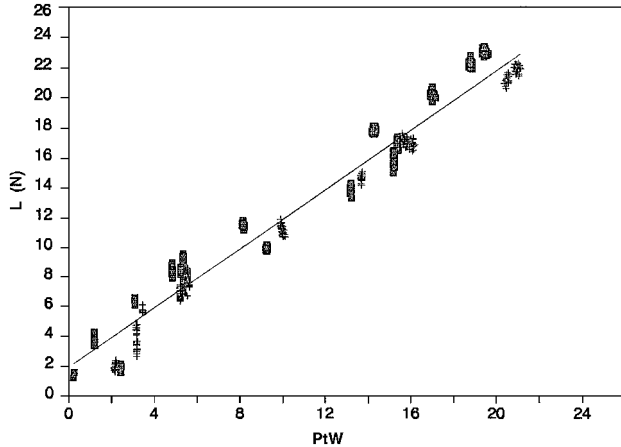
Parameter	Range
U , m/s	0 to 40
P , Pa	0 to 6000
t , mm	2 to 10

Table 8 Values of K_{1L} , K_{2L} , and K_{3L}

Test condition	K_{1L}	K_{2L}	K_{3L}	Correlation coefficient	Standard deviation, N
<i>With flap</i>					
$t = 2$ mm	0.582	-1.502	0.384	0.9961	1.785
$t = 6$ mm	0.759	3.562	0.224	0.9949	3.545
$t = 10$ mm	0.746	3.019	0.199	0.9937	3.464
$t = \text{all}$	0.771	3.215	0.200	0.9882	4.78
<i>No flap</i>					
$t = 2$ mm	-0.379	5.089	0.564	0.9905	4.728
$t = 6$ mm	0.127	1.488	0.604	0.9931	4.408
$t = 10$ mm	-0.217	6.419	0.227	0.9861	7.584
$t = \text{all}$	-0.314	3.555	0.577	0.9607	11.02

Table 9 Values of K_{1D} , K_{2D} , and K_{3D}

Test condition	K_{1D}	K_{2D}	K_{3D}	Correlation coefficient	Standard deviation, N
With flap	0.506	-0.259	0.206	0.9578	4.469
No flap	0.114	-1.175	0.258	0.6821	10.860

**Fig. 6** Variation of L with PtW for cylinders with and without a flap.

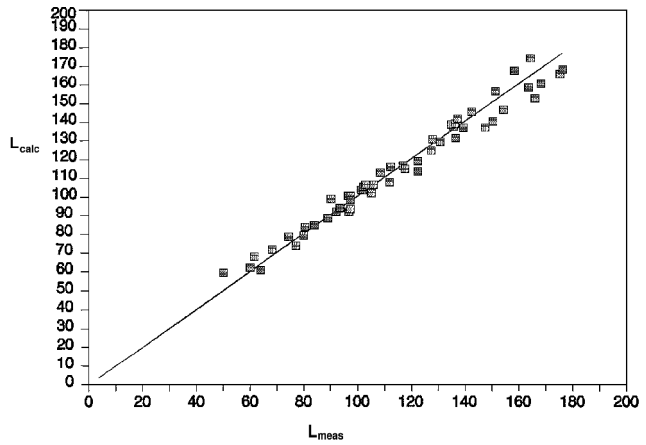
leaves the cylinder in a direction that is approximately parallel to the direction in which the lift acts. Thus a value of unity for K_{2L} is not a surprising result.

Lift and Drag due to Combined Freestream and Circulation Control Air

For the combined flow of freestream and CC air, the constants K_{1L} , K_{2L} , and K_{3L} for the cylinder, with and without, a flap can be obtained by means of multiple regression using Eq. (13). Similarly the constants K_{1D} , K_{2D} , and K_{3D} can be obtained using Eq. (14).

The ranges of the parameters over which the tests were carried out are given in Table 7. The tests were carried out with and without the flap fitted. The results obtained are presented in Table 8 for the lift and Table 9 for the drag and in Figs. 7, 8, and 9.

In Fig. 7 the lift calculated using Eq. (14) and the coefficients for $t = \text{all}$ given in Table 8 for a cylinder fitted with a flap are plotted against the measured values of lift. The corresponding data for a cylinder without a flap are presented in Fig. 8.

**Fig. 7** Variation of L_{calc} with L_{meas} (cylinder with flap).

Lift with a Flap

It can be seen from the data presented in Table 8 that for a CCC fitted with a flap the values of K_{1L} , K_{2L} , and K_{3L} remain fairly constant for slot thicknesses of 6 to 10 mm and for the combined case of slot thicknesses varying from 2 to 10 mm. In the absence of CC air, it was found that K_{1L} was a function of the slot thickness. For the combined flow the value of K_{1L} was similar to that obtained with no CC air indicating that the distortion of the flow caused by geometrical assymmetries is not strongly dependent on the presence of CC air.

The value of K_{2L} of 3.215 for the combined flow is larger than the value of approximately unity obtained when only CC air is used. The increase in K_{2L} can be attributed to a change of momentum of air from the freestream, which is entrained by the CC air as opposed to an increase in lift caused by the combined effects of circulation and freestream velocity.

Lift without a Flap

As was the case with no CC air, K_{1L} was found to be negative when the $t = 2$, 6, and 10 mm results are combined indicating that the flow distortion caused by the slots generates a negative lift as would be expected from the results obtained for the tests where the CC airflow was zero.

The value of K_{2L} for a cylinder without a flap is similar to that obtained for a cylinder with a flap, as was found to be the case for CC air alone tests. Because the value of K_{2L} for the combined flow case is similar to the value obtained for a cylinder with a flap, it may be expected that the momentum effects are similar for the two cylinders.

K_{3L} for a cylinder that is not fitted with a flap is higher than it is for a cylinder fitted with a flap. No reason for this is postulated except that the presence of a flap appears to promote circulation and increased lift.

It is clear from the results obtained that the lift generated by a CCC is indeed a function of three flow phenomena, and these should be taken into account when developing models to predict lift caused by CC.

Drag

The results obtained for the drag have not been presented in detail with only the values of K_{1D} , K_{2D} , and K_{3D} obtained for the combined flows being given in Table 9.

In Fig. 9 the drag calculated using Eq. (16) and the coefficients given in Table 9 for a cylinder fitted with a flap are plotted against the measured values of drag.

K_{1D} corresponds to the drag coefficient of a cylinder with no CC air divided by two. This coefficient is strongly dependent on the Reynolds number,⁴⁰ particularly in the Reynolds-number regime in which the tests were carried out. Thus the poor correlation obtained for the cylinder without a flap is not surprising. The effect of the flap, as indicated by the higher correlation coefficient for the cylinder

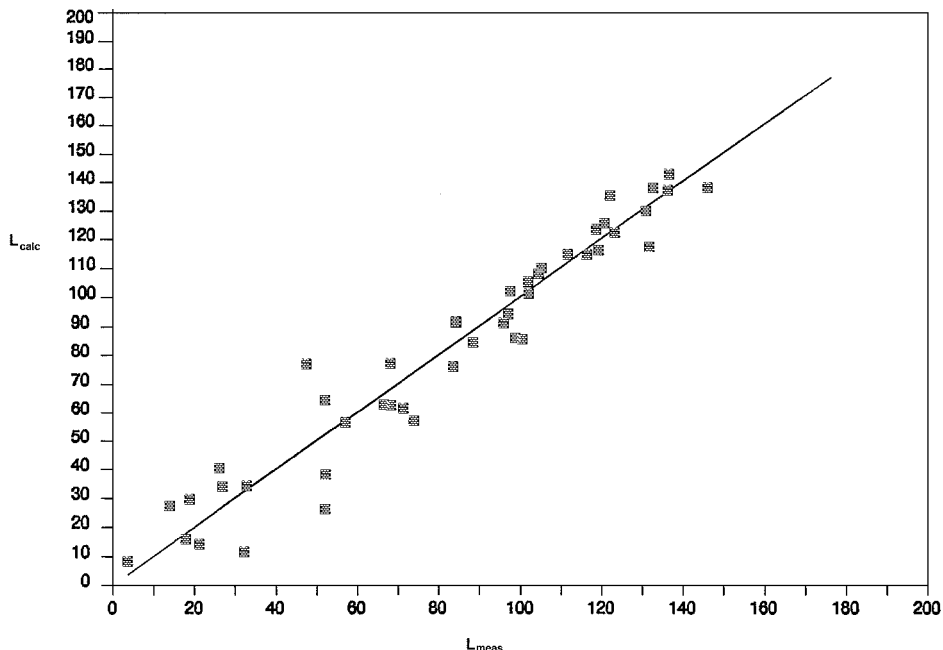


Fig. 8 Variation of L_{calc} with L_{meas} (cylinder with no flap).

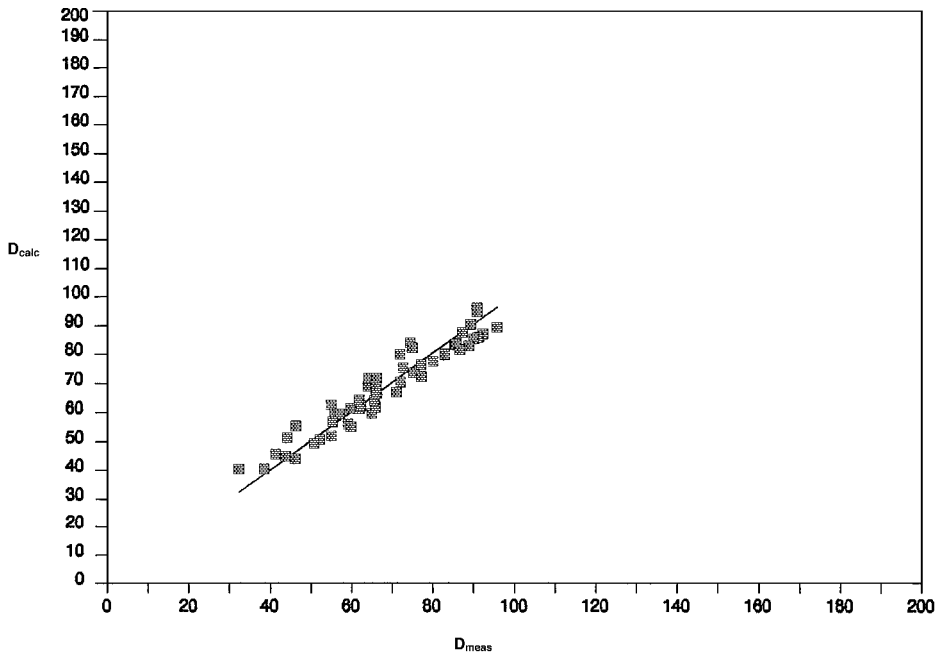


Fig. 9 Variation of D_{calc} with D_{meas} (cylinder with flap).

with a flap, is to stabilize the flow reducing the drag dependence on the Reynolds number.

The negative values of K_{2D} for both cylinders indicate that the change of momentum of the CC air results in a thrust acting on the cylinder. The magnitude of this thrust would depend on the angle at which the Coanda flow leaves the cylinder.

Positive values of K_{3D} indicate that a drag component exists, which is related to the lift attributed to the combined action of the circulation developed by the CC air and the freestream velocity. As the cylinder spanned the height of the tunnel and confirmed by the velocity profile downstream of the cylinder, it is unlikely that trailing vortices existed in the tunnel, and it can be concluded that this drag component results from the interaction of the flow streams and the resulting pressure distribution on the cylinder.

In general the lift of a CCC of the type tested can be predicted with greater accuracy than the drag as indicated by the higher correlation coefficients given in Tables 8 and 9 and the lower standard devia-

tions. The standard deviation of the lift is approximately 2.7% of the maximum lift of 180 N, whereas that of the drag is approximately 5.0% of the maximum drag of 90 N.

Conclusions

1) The lift and drag of a circulation controlled cylinder is comprised of three components, i.e., those caused by a) the distortion of the freestream by a nonsymmetrical cylinder; b) the momentum of the CC air; and c) the combined effects of the freestream and the CC flow, which generates a circulation around the cylinder.

2) The three components that contribute to the lift and drag are coupled over the domain of the tests.

3) The major component of the drag is caused by the flow of the freestream over the cylinder.

4) Surface irregularities tend to cause the flow to be deflected to the side of the cylinder on which the irregularities exist resulting in a contribution to the lift.

5) A flap has little effect on the lift associated solely with the momentum of the air.

6) A flap appears to result in a greater lift component attributable to the combined effects of circulation and freestream velocity.

Acknowledgments

Grateful thanks are extended to J. Cooper and the personnel of the workshop of the School of Mechanical Engineering for their contribution in the manufacture, installation, and upgrading of the adaptive wall wind tunnel.

References

¹Young, T., "Outlines of Experiments and Inquiries Respecting Sound and Light," *Royal Society Philosophical Transactions*, Vol. XC, Jan. 1800, pp. 604-626.

²Attinello, J. S., "Boundary Layer Control and Supercirculation," *Aeronautical Engineering Review*, Vol. 12, 1953.

³Donald, D. (ed.), *Take Off*, Vol. 1, Pt. 11, Eaglemoose Publications Ltd., London, 1993, pp. 300-307.

⁴Englar, R. J., Hemmerly, R. A., Moore, W. H., Seredinsky, V., Valckenaere, W., and Jackson, J. A., "Design of the Circulation Control Wing STOL Demonstrator Aircraft," *Journal of Aircraft*, Vol. 18, No. 1, 1981, pp. 51-58.

⁵Wilkerson, J. B., Reader, K. R., and Linck, D. W., "The Application of Circulation Control Aerodynamics to a Helicopter Rotor Model," *Journal of the American Helicopter Society*, Vol. 19, April 1974, pp. 1-16.

⁶Williams, R. M., "Application of Circulation Control Rotor Technology to a Stopped Rotor Aircraft Design," *Proceedings of the First European Rotorcraft and Powered Lift Aircraft Forum*, Southampton, England, U.K., Sept. 1975.

⁷Velazquez, J. L., "Advanced Anti-Torque Concepts Study (Lockheed California Company)," U.S. Army, USAAMDR TR 71-44, Aug. 1971.

⁸Logan, A. H., "Design and Flight Test of the No Tail Rotor (NOTAR) Aircraft," *Proceedings of the 38th Annual National Forum of the American Helicopter Society*, American Helicopter Society, Alexandria, VA, May 1982.

⁹Samapatacos, E., "MD Explorer Development and Test," *Proceedings of the Nineteenth European Rotorcraft Forum*, Cernobbio, Italy, Sept. 1993.

¹⁰Anikin, V. A., "Experimental Investigations in the Field of an Air Jet Nozzle Controlled Helicopter Aerodynamics," *Proceedings of the Eighteenth European Rotorcraft Forum*, Avignon, France, Sept. 1992.

¹¹Kind, R. J., and Maull, D., "An Experimental Investigation of a Low Speed Circulation Controlled Airfoil," *The Aeronautical Quarterly*, Vol. 19, May 1968, pp. 170-182.

¹²Englar, R. J., "Circulation Control for High Lift and Drag Generation on STOL Aircraft," *Journal of Aircraft*, Vol. 12, No. 5, 1975, pp. 457-463.

¹³Englar, R. J., "Development of an Advanced No-Moving-Parts High Lift Airfoil," *Congress of the International Council of the Aeronautical Sciences*, Seattle, Washington, Aug. 1982, pp. 951-959.

¹⁴Harvell, J. K., and Franke, M. E., "Aerodynamic Characteristics of a Circulation Control Elliptical Airfoil with Two Blown Jets," *Journal of Aircraft*, Vol. 22, No. 9, 1985, pp. 737-742.

¹⁵Novak, C. J., and Cornelius, K. C., "An LDV Investigation of a Circulation Control Airfoil Flowfield," AIAA Paper 86-0503, 1986.

¹⁶Fekete, G. I., "Coanda Flow of a Two-Dimensional Wall Jet on the Outside of a Circular Cylinder," McGill Univ., Montreal, Canada, Mech. Eng Research Labs. Rept. 63-112, 1963.

¹⁷Lockwood, V. E., "Lift Generation on a Circular Cylinder by Tangential Blowing from Surface Slots," NASA TN D-244, May 1960.

¹⁸Dunham, J., "Experiments Towards a Circulation-Controlled Lifting Rotor Part I—Wind Tunnel Tests," *Journal of the Royal Aeronautical Society*, Vol. 74, No. 678, 1970, pp. 91-103.

¹⁹Wilson, D. J., and Goldstein, R. J., "Turbulent Wall Jets with Cylindrical Streamwise Curvature," *Journal of Fluids Engineering*, Vol. 96, Sept. 1976, pp. 550-557.

²⁰Berndt, R. G., "Adaptive Wall Wind Tunnel Investigation of a Circulation Controlled Circular Cylinder," M.Sc. Thesis, School of Mechanical Engineering, Univ. of the Witwatersrand, Oct. 1992.

²¹Shakouchi, T., "Interaction Between Two-Dimensional Jet and Circular Cylinder (Effects of Ejection Angle)," *Proceedings of the 1st International Conference on Flow Interaction*, Hong Kong, Sept. 1994, pp. 571-574.

²²Schmidt, L. V., "Unsteady Aerodynamics of a Circulation Controlled Airfoil," *Proceedings of the Fourth European Rotorcraft Forum*, Stresa, Italy, Sept. 1978.

²³Cheeseman, I. C., and Seed, A. R., "The Application of Circulation Control by Blowing to Helicopter Rotor," *Journal of the Royal Aeronautical Society*, Vol. 71, No. 79, 1967, pp. 451-467.

²⁴Dunham, J., "Experiments Towards a Circulation-Controlled Lifting Rotor Part II—A Model Rotor," *Journal of the Royal Aeronautical Society*, Vol. 74, No. 679, 1970, pp. 175-186.

²⁵Logan, A. H., "Evaluation of a Circulation Control Tail Boom for Yaw Control," U.S. Army Research and Technology Lab., Rept. USARTL-TR-78-10, Fort Eustis, VA, April 1978.

²⁶van Horn, J. R., "NOTAR (No Tail Rotor) Hover Testing Using a Scale Model in Water," *Proceedings of the 42nd Annual Forum of the American Helicopter Society*, Washington, DC, June 1986, pp. 231-241.

²⁷Nurick, A., and Goosbeek, C., "Experimental and Computational Investigation of a Circulation Controlled Tail Boom," *Proceedings of the Eighteenth European Rotorcraft Forum*, Avignon, France, Sept. 1992.

²⁸Prouty, R. W., "NOTAR: Refining the Design," *Rotor and Wing*, March 1993, pp. 41, 42.

²⁹Spence, D. A., "The Lift Coefficient of a Thin Jet Flapped Wing," *Proceedings of the Royal Society A*, Vol. 238, 1956, pp. 46-68.

³⁰Dunham, L. A., "Theory of Circulation Control by Slot-Blowing Applied to a Circular Cylinder," *Journal of Fluid Mechanics*, Vol. 33, No. 3, 1968, pp. 495-514.

³¹Kind, R. J., "A Calculation Method for Circulation Control by Tangential Blowing Around a Bluff Trailing Edge," *The Aeronautical Quarterly*, Vol. 19, May 1968, pp. 205-223.

³²Gibbs, E. H., and Ness, N., "Analysis of Circulation Controlled Airfoils," *Journal of Aircraft*, Vol. 13, No. 2, 1976, pp. 158-160.

³³Dvorak, F. A., and Kind, R. J., "Analysis method for Viscous Flow over Circulation-Controlled Airfoils," *Journal of Aircraft*, Vol. 16, No. 1, 1979, pp. 23-28.

³⁴Tsze, C. T., Kidwell, G. H., and Vanderplaats, G. N., "Numerical Optimization of Circulation Control Airfoils," *Journal of Aircraft*, Vol. 19, No. 2, 1982, pp. 145-150.

³⁵Dvorak, F. A., and Choi, D. H., "Analysis of Circulation-Controlled Airfoils in Transonic Flow," *Journal of Aircraft*, Vol. 20, No. 4, 1983, pp. 331-337.

³⁶Soliman, M. M., Smith, R. V., and Cheeseman, I. C., "Modelling Circulation Control by Blowing," *Conference on Improvement of Aerodynamic Performance Through Boundary Layer Control and High Lift Systems*, 1984, pp. 7.1-7.10.

³⁷Sun, M., Pai, S. I., and Chopra, I., "Aerodynamic Force Calculations of an Elliptical Circulation Control Airfoil," *Journal of Aircraft*, Vol. 23, No. 9, 1986, pp. 673-680.

³⁸Shrewsbury, G. D., "Numerical Study of a Research Circulation Control Airfoil Using Navier-Stokes Methods," *Journal of Aircraft*, Vol. 26, No. 1, 1989, pp. 29-34.

³⁹Holz, R., Hassan, A., and Reed, H., "A 2-D Model for Predicting the Aerodynamic Performance of the NOTAR System Tailboom," *Proceedings of the 48th Annual Forum of the American Helicopter Society*, Washington, DC, June 1992, pp. 1295-1305.

⁴⁰Holz, R. G., and Hassan, A. A., "Numerical Model for Circulation Control Flows," *AIAA Journal*, Vol. 32, No. 4, 1994, pp. 701-707.

⁴¹Hoerner, S. F., *Fluid-Dynamic Drag* Sighard, Hoerner, Washington, DC, 1965, pp. 3-8, 3-9.